

1 The Abnormal Oswald Ripening of Protein Nanofiber in Myofibrillar
2 Protein Solution

3 Fuge Niu^{1†}, Rui Zhang^{1†}, Jiamei Fan¹, Weichun Pan^{1*}

4 ¹*The School of Food Science and Biotechnology, Zhejiang Gongshang University,*

5 *Xiasha Gaojiao Garden, Xuezheng Street 18, Hangzhou, China 310018*

6 [†] *Equal contribution*

7

8

9

10

11

12

13

14

15

16

17

18

19

20

21

22

23 Abstract: In solutions of myofibrillar protein extracted from giant squid (*Dosidicus*
24 *gigas*), the size-coarsening process of protein nanofiber is complex. At high
25 temperature (25°C), nanofiber keeps growth but with two distinguishable patterns,
26 slow rate at the initial stage with $t^{0.2}$ and the fast one at the late stage with $t^{2.3}$. The
27 intersection of these two slopes is around 300 min. Meanwhile, protein concentration
28 in solution enhances as well. These behaviors contradict to the prediction of Ostwald
29 ripening. Thus, we call this process as abnormal. These abnormal behaviors come
30 from the conformation change of some types of constitution protein molecules with
31 chemical potential reduction when they dissolve from nanofiber to solution. On the
32 other hand, low temperature (10°C) depresses this size growth. This observation
33 suggests that temperature regulates protein molecule conformation change in
34 nanofiber. The consequence of this abnormal Ostwald ripening process is that all
35 protein molecules in nanofiber are redistributed. Protein molecules with the absence
36 of conformation change in dissolution accumulate in nanofiber to cause it growing,
37 while the rest concentrates in solution.

38 Keywords: Abnormal Ostwald ripening, myofibrillar protein, molecular conformation
39 change, nanofiber

40
41
42
43
44
45
46
47
48
49

50 In 1896 Wilhelm Ostwald described the phenomenon of large particle growth in
51 the cost of small one as Ostwald ripening due to the surface tension which is
52 proportional to the particles curvature(1-3). *As a result, the solute concentration keeps*
53 *reduction throughout size-coarsening process.* Meanwhile, an essential prerequisite,
54 no molecular conformation change when a molecule transfers from one phase to
55 another, exists but is always ignored. This condition is satisfied in inorganic and
56 organic compounds. However, in protein solutions containing particles with various
57 sizes, it should be cautious to apply Ostwald ripening theory in the size-coarsening
58 process because protein molecules are sensitive to the ambient conditions. Even salt
59 concentration variation could induce protein molecule conformation change(4). Thus,
60 *it is worth to verify Ostwald ripening theory in protein solutions.*

61 The existence of nanofiber in solutions of myofibrillar protein extracted from
62 giant squid (*Dosidicus gigas*) is verified(5). In order to investigate its size-coarsening
63 process in this solution, 2.73 mg mL⁻¹ myofibrillar protein was diluted 10 times by the
64 buffer solution, and was assessed by the dynamic light scattering (DLS) technique and
65 the fluorescence spectroscopy (FS) technique immediately.

66 In Fig. 1a, the pattern of light intensity on time depends on the temperature. High
67 temperature (25°C) allows the light intensity monotonically growing, while low
68 temperature (10°C) depresses this growth with almost constant light intensity
69 throughout the experiment. Due to high activity of enzymolysis in myofibrillar protein
70 at 25°C(6), it is necessary to estimate its influence in this study. In Fig. 1b, the
71 apparent concentrations of myofibrillar protein in three cases were determined via

72 Bradford protein assay. It displaces two issues: 1) the apparent protein concentration
73 remarkable increase overnight no matter whether ethylenediaminetetra acetic acid
74 (EDTA) is present or absent; 2) the existence of EDTA has minor effect on the
75 apparent concentration determinations. Since EDTA is a efficient agent to depress
76 enzymolysis(7), it could be concluded that the effect of enzymolysis could be ignored
77 in this study.

78 Another issue of interest in Fig. 1b is the apparent concentration rising with time.
79 Ref. 5 illustrates that the apparent concentration increase via Bradford protein assay
80 hints the more surface of protein molecule exploring to the solvent. In other words,
81 nanofiber dissolves into several pieces with small size. However, the last stage of light
82 intensity observation with fast increase at 25°C in Fig. 1a is against this prediction
83 because the light intensity is proportional to the particle number density and is
84 six-power of the size of particle(8). The light intensity increment due to the number
85 density increase is much smaller than its reduction due to the size shrinking during the
86 dissolution process. In order to clarify this puzzle, the size of corresponding nanofiber
87 was evaluated via DLS technique. Fig. 1c reveals that the decay of the autocorrelation
88 function $g_2(\tau)-1$ becomes slow throughout the experiment. With the aid of Laplace
89 transform, the corresponding decay time distribution was obtained (Fig. S1). The
90 decay time of the slow mode τ was assessed to construct Fig. S2. In contrast to the
91 case in 10°C in which τ is almost constant throughout experiment (data do not
92 present), the dependency of τ on the observation time has two patterns, $t^{0.2}$ and $t^{2.3}$,
93 with the intersection of these two slopes around 300 min (Fig. S2). In the initial stage

94 of size-coarsening process, 0.2 is close to the value in phase-separation process,
95 0.212(9, 10). But in the second stage, to the best of our knowledge, 2.3 is larger than
96 any reported value(11, 12) .

97 Now there is a problem. On the one hand, nanofiber keeps growth. On the other
98 hand, protein concentration in solution increases as well, which contradicts to the
99 prediction of Ostwald ripening. How does this phenomenon occur? Hinted by the fact
100 of tropomyosin (Fig. S3) dissolution from F-actin with the expense of partial
101 degradation of helical structure(13), we hypothesized this abnormal Ostwald ripening
102 due to some types of protein molecule conformation change when these molecules
103 dissolve from nanofiber to solution with chemical potential reduction. As a result,
104 these types of protein molecules concentrate in solutions. In order to verify the
105 hypothesis of protein molecule conformation change, FS technique was carried out
106 immediately after 2.15 mg mL^{-1} myofibrillar protein solution was diluted 10 times.
107 The reason to pick up FS is the high sensitivity of tryptophan to the local environment
108 in intrinsic protein florescence. As a result, change in the emission spectrum of
109 tryptophan is utilized to probe protein conformation change(14, 15). Especially for
110 minor change without secondary structure modification, such as the case of this study,
111 the traditional techniques, such as circular dichroism (CD), are infeasible. The
112 florescent spectra of the corresponding solution at various intervals were displayed in
113 Fig. 1d, in which the fluorescent light intensity keeps reduction with maximum of
114 fluorescent spectra shifting from 309 nm to 307 nm. This observation indicates the
115 occurrence of conformation change of protein molecules. In addition, the interval of

116 remarkable fluorescent light intensity reduction, around 5 h, coincides with the
117 intersection of the two slopes in Fig. S2.

118 Thus, at 25°C the slow growth rate of nanofiber at the initial stage (Fig. S1) may
119 come from the fact of high activation energy for protein molecule conformation
120 change, for instance, 430-490 kJ mol⁻¹ for ovalbumin at pH 7⁽¹⁶⁾.

121 But what factors do dominate protein molecule conformation change? Fig. 1a hints
122 that it is temperature rather than protein molecule concentration. When temperature is
123 low as 10°C, nanofiber is stable, which is partially verified by the fact of animal
124 muscles with less muscle shortening and drip loss around 10~15°C(17, 18). Only is
125 temperature high, such as 25°C, some types of protein molecules commencing
126 molecular conformation change when they redistribute from nanofiber to solution in
127 myofibrillar protein. Indeed, it is found that the tropomyosin dissociation from F-actin
128 has a minimum temperature of 35-40°C(19).

129 The aforementioned discussions lead to a prediction that in size-coarsening process
130 protein molecules with the absence of conformation change when dissolving from
131 nanofiber to solution accumulate to nanofiber while the rest types are condensed in
132 the solution. In other words, the compositions of solution and nanofiber respectively
133 become purer after this size-coarsening process, which was tested by the differential
134 scanning calorimetry (DSC) assessment (Fig. 2 and Table 2), in which solutions with
135 2.71 mg mL⁻¹ and 0.26 mg mL⁻¹ respectively were assessed. The dilution operation
136 induces the size-coarsening process in myofibrillar protein solutions. Compared with
137 the high concentration solution, the peak is sharp in the thermogram with the low

138 denatured temperature and less denatured enthalpy in low concentration solution. The
139 sharp peak indicates the purer composition in nanofiber(20). In addition, the dilution
140 operation causes nanofiber loose, corroborated by fractal dimension d_f assessment
141 with monotonic reduction (Fig S4 and Table S1). This may be the reason for low
142 denatured temperature and less denatured enthalpy in the low concentration solution.

143 From the aforementioned discussion, a crucial conclusion is made that protein
144 molecule conformation change is an essential prerequisite for muscle protein
145 dissolution from the solid state to solution. In addition, this conformation change
146 process is regulated by temperature rather than protein molecule concentration. Just
147 because many food additives have strong interactions with muscle protein molecules,
148 they can significantly affect muscle protein molecules dissolution and thereby can
149 influence the properties of final products made by muscle (21, 22). This observation
150 also sheds light on clinical practices, for instance, the mechanism study of
151 rhabdomyolysis, a complex process associated with morbidity and mortality(23).

152

153 **SUPPORTING MATERIAL**

154 Supporting Materials and Methods, five figures, and one table are available.

155 **AUTHOR CONTRIBUTIONS**

156 F. N. and R. Z. have equal contribution in this study. F. N., R. Z., and J. F. carried out
157 the experiments. W. P. designed the study. F. N., R. Z. and W. P. analyzed the data,
158 discussed and interpreted results. W. P. wrote the manuscript.

159 **ACKNOWLEDGEMENTS**

160 The authors wish to thank Dr. Peter G. Vekilov of University of Houston for many
161 helpful comments and criticisms. This work was supported by grants from the
162 National Natural Science Foundation of China (31171713, 31701650), the Foundation
163 of Food Science and Engineering, the Most Important Discipline of Zhejiang Province
164 (JYTsp20142014), The Natural Science Foundation of Zhejiang Province
165 (LY17C200004).

166 The authors declare that they have no known competing financial interests or personal
167 relationships that could have appeared to influence the work reported in this paper.

168 **SUPPORTING CITATIONS**

169 References (24–30) appear in the Supporting Material.

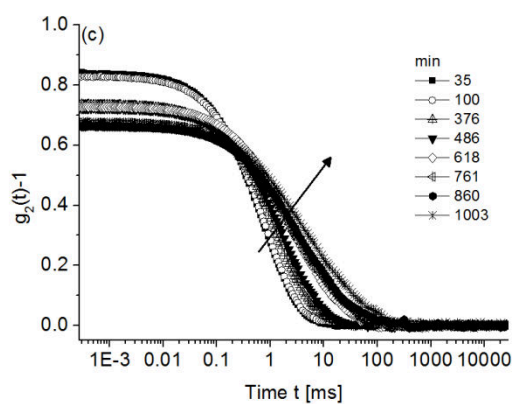
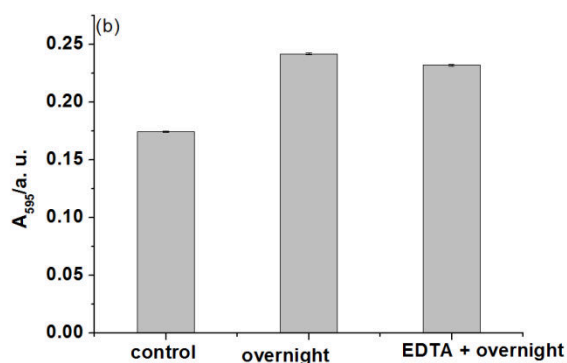
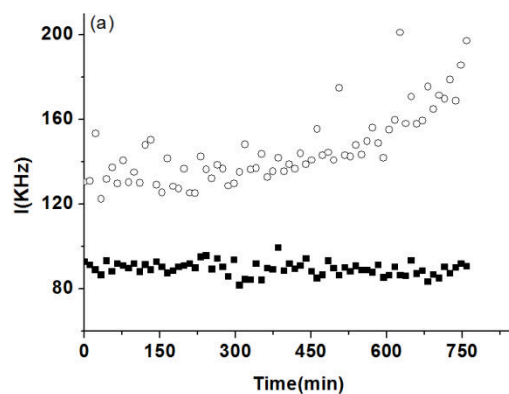
170

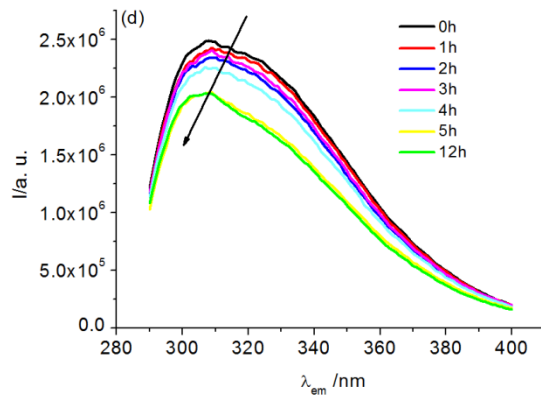
171 **REFERENCES**

- 172 1. Ostwald, W. 1896. Lehrbuch der Allgemeinen Chemie, Leipzig, Germany.
- 173 2. Ostwald, W. 1897. Studien über die Bildung und Umwandlung fester Körper. Z. Phys. Chem.
174 22:289-330.
- 175 3. Ratke, L., and P. W. Voorhees. 2002. Growth and Coarsening Ostwald Ripening in Material
176 Processing. Springer-Verlag Berlin Heidelberg, Berlin, Germany.
- 177 4. Zhang, R., R. Zhou, W. Pan, W. Lin, X. Zhang, M. Li, J. Li, F. Niu, and A. Li. 2017. Salting-in effect
178 on muscle protein extracted from giant squid (*Dosidicus gigas*). Food Chem. 215:256-262.
- 179 5. Niu, F., R. Zhang, J. Fan, W. Pan, and A. Li. submitted The Existence of Nanofiber in Solutions
180 of Myofibrillar Protein Extracted from Giant Squid (*Dosidicus gigas*). submitted.
- 181 6. Gomez-Guillén, M. C., J. L. Hurtado, and P. Montero. 2002. Autolysis and protease inhibition
182 effects on dynamic viscoelastic properties during thermal gelation of squid muscle. J. Food Sci.
183 67:2491-2496.
- 184 7. Konno, K., C. Young-Je, T. Yoshioka, P. Shinho, and N. Seki. 2003. Thermal denaturation and
185 autolysis profiles of myofibrillar proteins of mantle muscle of jumbo squid *Dosidicus gigas*.
186 Fish. Sci. 69:204-209.
- 187 8. Schärftl, W. 2007. Light Scattering from Polymer Solutions and Nanoparticle Dispersions.
188 Springer, Leipzig, Germany.
- 189 9. Langer, J. S. 1975. Spinodal Decomposition. Fluctuations, Instabilities, and Phase Transitions. T.
190 Riste, editor. Springer-Verlag US Boston, MA, USA, pp. 19-42.
- 191 10. Langer, J. S., M. Bar-on, and H. D. Miller. 1975. New computational method in the theory of

- 192 spinodal decomposition. Phys. Rev. A 11:1417-1429.
- 193 11. Shi, B. Q., C. Harrison, and A. Cumming. 1993. Fast-Mode Kinetics in Surface-Mediated
194 Phase-Separating Fluids. Phys. Rev. Lett. 70:206-209.
- 195 12. Tanaka, H., and T. Araki. 1998. Spontaneous Double Phase Separation Induced by Rapid
196 Hydrodynamic Coarsening in Two-Dimensional Fluid Mixtures. Phys. Rev. Lett. 81:389-392.
- 197 13. Tanaka, H. 1972. The helix content of tropomyosin and the interaction between tropomyosin
198 and F-actin under various conditions. Biochim. Biophys. Acta Protein Structure 278:556-566.
- 199 14. Lakowicz, J. R. 2006. Principles of Fluorescence Spectroscopy. Springer Science + Business
200 Media, LLC, New York, NY, USA.
- 201 15. D'Auria, S., M. Staiano, I. M. Kuznetsova, and K. K.Turoverov. 2005. The combined use of
202 fluorescence spectroscopy and x-ray crystallography greatly contributes to elucidating
203 structure and dynamics of proteins. Reviews in Fluorescence. C. D. Geddes and J. R. Lakowicz,
204 editors. Springer US, New York, USA, pp. 25-61.
- 205 16. Weijers, M., P. A. Barneveld, M. A. C. Stuart, and R. W. Visschers. 2003. Heat-induced
206 denaturation and aggregation of ovalbumin at neutral pH described by irreversible first-order
207 kinetics. Protein Sci. 12:2693–2703.
- 208 17. Honikel, K. O., C. J. Kim, and R. Hamm. 1986. Sarcomere Shortening of Prerigor Muscles and
209 Its Influence on Drip Loss Meat Sci. 16:267-282.
- 210 18. Lesiak, M. T., D. G. Olson, C. A. Lesiak, and D. U. Ahn. 1996. Effects of Postmortem
211 Temperature and Time on the WaterHolding Capacity of Hot-Boned Turkey Breast and Thigh
212 Muscle. Meat Sci. 43:51-60.
- 213 19. Tanaka, H., and F. Oosawa. 1971. The effect of temperature on the interaction between
214 F-actin and tropomyosin. Biochim. Biophys. Acta Bioenerg 253:274-283.
- 215 20. Chiu, M. H., and E. J. Prenner. 2011. Differential scanning calorimetry: An invaluable tool for a
216 detailed thermodynamic characterization of macromolecules and their interactions. J. Pharm.
217 Bioallied Sci. 3:39-59.
- 218 21. Sánchez-Alonso, I., M. T. Solas, and A. J. Borderías. 2007. Technological implications of
219 addition of wheat dietary fibre to giant squid (*Dosidicus gigas*) surimi gels. J. Food Eng.
220 81:404-411.
- 221 22. Gómez-Guillén, M. C., and A. J. B. P. Montero. 1997. Salt, Nonmuscle Proteins, and
222 Hydrocolloids Affecting Rigidity Changes during Gelation of Giant Squid (*Dosidicus gigas*). J.
223 Agric. Food Chem. 45:616–621.
- 224 23. Torres, P. A., J. A. Helmstetter, A. M. Kaye, and A. D. Kaye. 2015. Rhabdomyolysis:
225 Pathogenesis, Diagnosis, and Treatment. Ochsner J. 15:58-69.
- 226 24. Hashimoto, K., S. Watabe, M. Kono, and K. Shiro. 1979. Muscle protein composition of sardine
227 and mackerel. Bull. Jpn Soc. Sci. Fish. 45:1435-1441.
- 228 25. Konno, K., C. Young-Je, T. Yoshioka, P. Shinho, and N. Seki. 2003. Thermal denaturation and
229 autolysis profiles of myofibrillar proteins of mantle muscle of jumbo squid *Dosidicus gigas*.
230 Fish. Sci. 69:204-209.
- 231 26. Bradford, M. M. 1976. A Rapid and Sensitive Method for the Quantitation of Microgram
232 Quantities of Protein Utilizing the Principle of Protein-Dye Binding Anal. Biochem.
233 72:248-254.
- 234 27. Schatzel, K. 1993. Single-photon correlation techniques. Dynamic Light Scattering: The
235 Method and Some Applications W. Brown, editor. Clarendon Press, Oxford, pp. 76-148.

- 236 28. Provencher, S. W. 1982. A constrained regularization method for inverting data represented
237 by linear algebraic or integral equations. *Comput. Phys. Commun.* 27(3):213-324.
- 238 29. Provencher, S. W. 1982. CONTIN: A general purpose constrained regularization program for
239 inverting noisy linear algebraic and integral equations. *Comput. Phys. Commun.*
240 27(3):229-242.
- 241 30. Lin, M. Y., H. M. Lindsay, D. A. Weitz, R. C. Ball, R. Klein, and P. Meakin. 1989. Universality in
242 colloid aggregation. *Nature* 339:360-363.
- 243



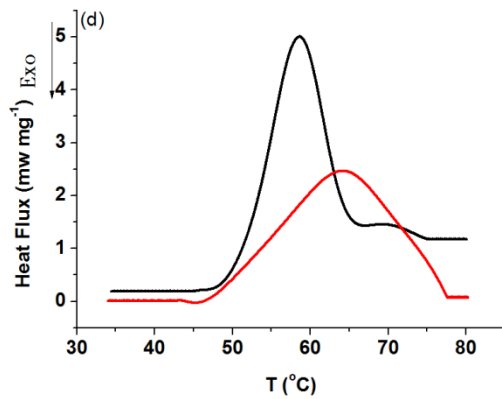


247

248 Figure 1 (a) Time evolutions of light intensity at various temperatures. Empty circle
249 stands for 25°C with 0.27 mg mL^{-1} myofibrillar protein while solid square does for
250 10°C at the same protein concentration. (b) The influence of enzyme on protein
251 concentration assessment in myofibrillar protein solutions. The control is 0.27 mg
252 mL^{-1} myofibrillar protein solution. While the middle one is the solution same as
253 control but has stayed in a heat bath at 25°C overnight; and the right one is a sample
254 same as the middle one but added EDTA to depress enzyme activity. The Bradford
255 method was applied for absorbance determination. (C)The autocorrelation functions
256 of DLS at 25 °C in Fig.1a at some intervals. (d) The fluorescence emission spectrums
257 at various intervals, which displace light intensity reduction and maximum of
258 fluorescent spectra shifting from 309 nm to 307 nm.

259

260



261

262 Figure 2. DSC determinations of myofibrillar protein solutions at two concentrations
263 2.71 mg mL⁻¹ (black line) and 0.26 mg mL⁻¹ (red line).

264

265

Table 1 The thermal stability of particles under various dilution ratios

Dilution ratio	T _{max} (°C)	ΔH (J/s)
1	63.9 ^a	0.529 ^a
10	58.6 ^b	0.362 ^b

266 T_{max}, the denaturation temperature; ΔH, the endotherm enthalpy. Different letters (a-b) indicate
267 significant (P < 0.05) difference within the same row.

268